Journal of Hazardous Materials 189 (2011) 265–272

Contents lists available at ScienceDirect

Journal of Hazardous Materials

journal homepage: www.elsevier.com/locate/jhazmat

Adsorption behavior of Cu(II) onto titanate nanofibers prepared by alkali treatment

Nian Li, Lide Zhang*, Yongzhou Chen, Yue Tian, Huimin Wang

Key Laboratory of Materials Physics, Anhui Key laboratory of Nanomaterials and Nanostructure, Institute of Solid State Physics, Chinese Academy of Sciences, Hefei 230031, PR China

ARTICLE INFO

Article history:
Received 2 December 2010
Received in revised form 18 January 2011
Accepted 11 February 2011
Available online 17 February 2011

Keywords:
Titanate nanofibers
Cu(II) adsorption
Isotherms
Kinetics

ABSTRACT

Novel low-cost adsorbents of titanate nanofibers with formula $Na_xH_{2-x}Ti_3O_7{\cdot}nH_2O$ have been prepared by alkali treatment for Cu(II) removal from aqueous solutions. The nanofibers have structures in which three edge-shared TiO_6 octahedras join at the corners to form stepped, zigzag $Ti_3O_7^{2-}$ layers. The sodium cations located between the layers are exchangeable. The results of batch adsorption experiments suggest that the nanofibers with high sodium content can be effective adsorbents for Cu(II) removal. Effects of several important factors such as Na amount in adsorbents, pH, temperature, contact time and initial concentration are systematically studied. Results show that the adsorption is highly pH-dependent and the removal is almost complete (99.8%) for initial concentration under 100 mg/l at pH 4. Equilibrium adsorption follows Langmuir isotherms well and the maximum Cu(II) uptake calculated is 167.224 mg/g. The adsorption kinetics can be explained by pseudo-second-order model well and the time needed for equilibrium is 180 min. Thermodynamic study indicates that the adsorption is spontaneous and endothermic. Desorption of Cu(II) from adsorbents using EDTA-2Na solutions exhibits a high efficiency and the adsorbents can be used repeatedly. These results demonstrate that the titanate nanofibers are readily prepared, enabling promising applications for the removal of Cu(II) from aqueous solutions.

1. Introduction

The ever-increasing contamination of water by heavy metal ions has become a serious environment problem. Heavy metals discarded from industrial waste are highly toxic at relatively low concentrations and can cause several disorders and diseases in human beings when tolerance levels are exceeded [1–3]. The removal of these heavy metal ions from dilute or concentrated solutions has been of great concern because they are not biodegradable and their accumulation in living tissues throughout the food chain [4].

Copper, which has many applications in industries, is one of the most important toxic heavy metals. It can cause serious problems to human beings such as stomach intestinal distress, kidney damage, anemia and even coma and eventual death [5]. In China, according to the newly issued National Drinking Water Standard [6], the limit of copper concentration in drinking water is 1.0 mg/l. It is important to develop technologies that can be large-scale used for copper removal. Several methods including chemical precipitation, membrane filtration, ion exchange, liquid extraction, electro deposition and adsorption [7–9] have been reported. Among all these methods, the adsorption technique is by far the most versatile and widely used due to its relatively low cost and high feasibility for industrial application. The most common adsorbent materials are activated carbon [10], alumina silica [11], metal hydroxides [12] and biosorption materials [13]. But most of these materials suffer from severe constraints, such as incomplete metal removal, complex procedure, high cost and low efficiency. Therefore some new high effective adsorbent materials that could be large-scale used in industries should be explored.

Recently, nanomaterials are special attractive in the searching of high effective adsorbents for heavy metal removal due to their unique chemical and physical properties [14]. Mesoporous titanate nanostructures obtained by alkali treatment have attracted a great deal of attention since the innovative work of Kasuga et al. [15,16]. These materials can be easily synthesized by hydrothermal treatment of crystalline TiO_2 in highly concentrated alkaline solutions at moderate temperatures (60–210 °C). The preparation conditions such as alkali concentrations, reaction time and temperatures can be easily adjusted to obtain different nanoshaped mesoporous titanates (such as nanotubes, nanofibers, nanoribbons and nanowires) [17–23]. They have structures in which TiO_6 octahedra join each other to form layers with negative charges and Na^+ ions existing within the layers are ion exchangeable [22]. The nanostructured titanates have been successfully used in many applications, such as photocatalysts [24,25], hydrogen storage [26]

* Corresponding author. Tel.: +86 551 5591420; fax: +86 551 5591434.
E-mail address: ldzhang@issp.ac.cn (L. Zhang).

0304-3894/$ – see front matter © 2011 Elsevier B.V. All rights reserved.
doi:10.1016/j.jhazmat.2011.02.031

and lithium batteries [27,28]. Due to the cation exchange ability [17] and large surface area [29], they also have the potential to be used as effective adsorbents for heavy metal removal from wastewater. Up to the present, most of the studies of nanostructured titanates are focused on the fabrication and characterization, only a few on the use of heavy metal recovery. Chen et al. [30] found that titanate nanotubes were effective in adsorbing Pb(II). Liu et al. [31] demonstrated that Cu(II) adsorption on titanate nanotubes was highly dependent on Na content. Niu et al. [32] found that the maximum uptake of As(V) and As(III) by titanate nanotubes was 208 mg/g and 60 mg/g, respectively. The equipments required to synthesize nanostructured titanates are simple and alkali solutions are reusable, hence the adsorbents have the potential to be large-scale used. However, all the titanates they used for heavy metal removal had tubular structures and Degussa P25 (a mixture powder of ~80% anatase and ~20% rutile) was used as Ti precursor. Considering the fact that synthesis conditions for nanotubes are relatively strict and Degussa P25 is not an ideal precursor for low cost adsorbents due to its high price, we assume that the heavy metal removal ability of titanates is not dependent on the tubular structure and titanates with other morphologies such as nanofibers can still have the same adsorption capacity as nanotubes or even better. The conditions to synthesize titanate nanofibers are much looser and many kinds of Ti precursors even the industrial grade minerals [33] can be used.

In this study, industrial grade metatitanic acid is used as Ti precursor, and titanate nanofibers (TNFs) are synthesized as the novel adsorbents. It is worth noting that the cost of industrial grade metatitanic acid used here is about US1.5$/kg, which is 1/20–1/100 of a commercial TiO_2 powder (anatase, rutile or Degussa P25). The objective of this study is to investigate the possible use of the TNFs as alternate adsorbents for the removal of Cu(II) from wastewater. The TNFs are characterized by XRD, SEM, BET and EDX. Batch experiments are carried out for the study on Cu(II) removal from aqueous solutions. The influence of several important parameters such as Na amount in TNFs, initial pH of Cu(II) solutions, temperature, contact time and initial Cu(II) concentration is investigated. The Langmuir and Freundlich isotherm models are used to fit the experimental data. Pseudo-first-order and pseudo-second-order kinetic models are used to evaluate the kinetics of adsorption. Desorption study is performed and adsorption mechanism is then discussed.

2. Experimental

2.1. Materials

Simulated aqueous solutions containing Cu(II) were prepared by dissolution of copper nitrate in deionized water. Metatitanic acid ($TiO(OH)_2$, TiO_2 content 80%) was purchased from Shanghai Mintchem Development Co., Ltd. and used without any further purification. $Cu(NO_3)_2$, NaOH, HCl and EDTA-2Na of AR grade were used. All water used in this study had been treated by the deionized water equipment.

2.2. Synthesis of titanate nanofibers

The titanate nanofibers (TNFs) were prepared through the hydrothermal method. In a typical synthetic procedure, 2 g metatitanic acid was mixed with 40 ml 10 M NaOH solution in a 50 ml Teflon-lined autoclave container. The mixture was stirred to form a milk-like suspension, sealed and hydrothermal treated at 160 °C for 24 h. After hydrothermal reaction, the precipitate was separated by filtration and washed with water or with an HCl solution at different concentrations (0.001 M, 0.01 M and 0.1 M) for several times and then dried overnight at 80 °C in air. The purpose of the acid washing process was to control Na amount in samples through ion exchange between Na^+ and H^+. For convenience, we denoted the TNFs treated with water, 0.001 M HCl, 0.01 M HCl and 0.1 M HCl as TNFs-1, TNFs-2, TNFs-3 and TNFs-4, respectively.

2.3. Characterization tools

X-ray diffraction (XRD) analyses were performed on a powder diffractometer (X'Pert Pro MPD) with Cu Kα (λ = 1.5406 Å) radiation. The morphology of the samples was determined by field emission scanning electron microscopy (FESEM, FEI Sirion-200). Energy dispersive X-ray (EDX, Inca Oxford) analysis was performed to determine the elemental composition of TNFs before and after adsorption. The zeta potential of TNFs was measured using the Zeta-Meter (zetasizer 3000HSA, Malvern). Cu(II) concentrations were measured by Inductively Coupled Plasma Spectrometer (Thermo Scientific iCAP 6000).

2.4. Adsorption experiments

The adsorption of Cu(II) on TNFs was studied by the batch technique. A thermostatic incubator shaker (TS-100B, Tensuc Shanghai) was used for adsorption experiments. The general method used for this study is described as follows: 50 mg TNFs were equilibrated with 40 ml Cu(II) solution in a stoppered glass flask at a fixed temperature and stirring speed. After adsorption, the phases were separated by filtration and the filtrate was collected for Cu(II) concentration measurements by ICP Spectrometer. To maximize the efficiency of Cu(II) removal by TNFs, each important factor (Na amount in TNFs, pH, temperature, contact time and initial Cu(II) concentration) was studied separately while other factors were kept constant.

For Na amount effect, TNFs-1, TNFs-2, TNFs-3 or TNFs-4 each with a dose of 50 mg were mixed with a 40 ml 100 mg/l Cu(II) solution. The solutions were agitated at a speed of 300 rpm and at a temperature of 30 °C for 6 h. Only the TNFs with the best Cu(II) removal (TNFs-1) would be used in the subsequent study.

For initial pH effect, a serious of 40 ml 100 mg/l Cu(II) solutions with different pH values from 1.0 to 7.0 were prepared. Solutions of 0.1 M NaOH and HCl were used for pH adjustment. A PHS-3C pH meter was used to determine pH of solutions. Each solution was mixed with 50 mg TNFs-1, and then agitated at a speed of 300 rpm and at a temperature of 30 °C for 6 h. Only the optimum pH would be used in the further study.

The effects of temperature, initial concentration and contact time were investigated using the same method as above. All the experiments were duplicated and only the mean values were reported. The maximum deviation observed was less than ±5%.

The amount of Cu(II) adsorbed q_t (mg/g) at time t (min), adsorption capacity q_e (mg/g) at equilibrium and the Cu(II) removal percentage were calculated as follows:

$$q_t = \frac{(C_0 - C_t)V}{W} \quad (1)$$

$$q_e = \frac{(C_0 - C_e)V}{W} \quad (2)$$

$$\%\text{Removal of Cu(II)} = 100 \times \frac{C_0 - C_e}{C_0} \quad (3)$$

where C_0 (mg/l), C_t (mg/l) and C_e (mg/l) are concentrations at initial, time t and equilibrium, respectively, V (ml) is the volume of Cu(II) solution and W (mg) is the total amount of TNFs.

2.5. Desorption experiments

Desorption of Cu(II) from TNFs-1 was examined using EDTA-2Na solutions of different concentrations. 50 mg TNFs-1 were first equi-

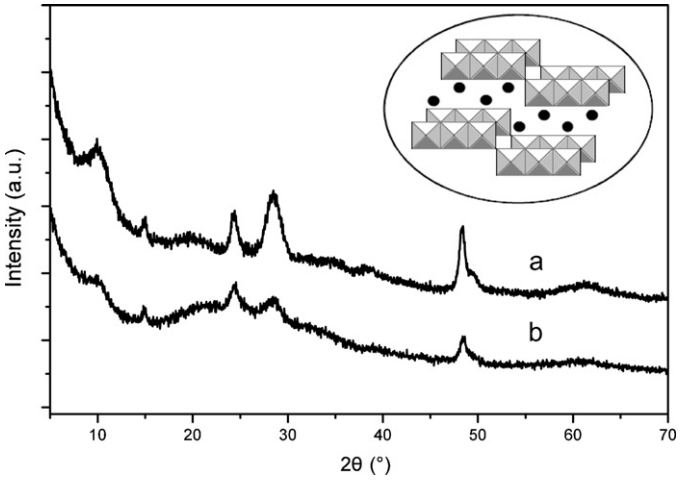

Fig. 1. XRD patterns of TNFs-1 before (a) and after (b) adsorption. Insert: schematic diagram of the structures of the TNFs-1.

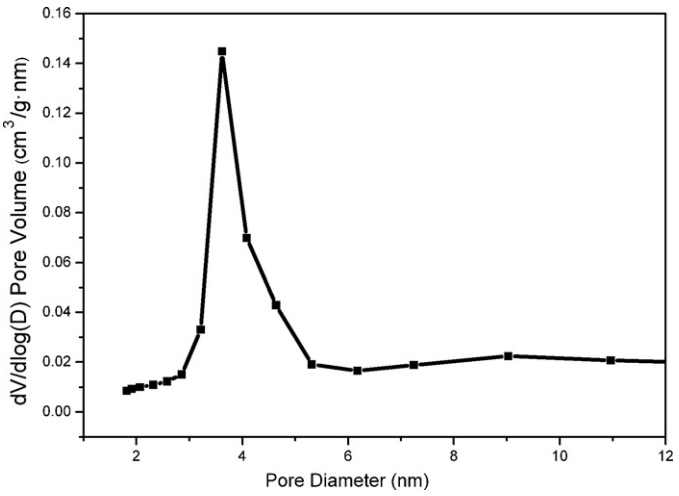

Fig. 3. Pore size distribution of TNF-1.

librated with a 40 ml Cu(II) solution with an initial concentration of 100 mg/l at pH 4 for an adequate time. After the adsorption, TNFs-1 with Cu(II) loaded were filtrated out and dried at 80 °C overnight. Then, the Cu(II) loaded TNFs-1 were added into 50 ml of the desorption solution with controlled concentration (10^{-1}–10^{-4} M). The mixture was stirred at 300 rpm, 30 °C for 2 h. The samples were taken from the solution and the supernate was sent to monitor the amount of Cu(II) ions desorbed into the solution. After the desorption test, the TNFs-1 were washed with deionized water and dried at 80 °C overnight, and then reused in the next cycle of adsorption experiment.

3. Results and discussion

3.1. Characterization of samples

Fig. 1 shows the XRD patterns of TNFs-1 before and after adsorption. The main diffraction peaks of TNFs-1 are typical of layered titanates, especially the one around $2\theta = 10^{\circ}$, attributed to the interlayer distance in $Na_xH_{2-x}Ti_3O_7{\cdot}nH_2O$ [34–37]. The position of this peak slightly shifts after adsorption, which may due to the change of interlayer distance after Na^+ ions are replaced by Cu^{2+} ions. Schematic diagram of the structures of $Na_xH_{2-x}Ti_3O_7{\cdot}nH_2O$ is also shown in Fig. 1. As can be seen, three edge-shared TiO_6 octahedras join at the corners to form a stepped, zigzag layered structure. Na^+, H^+ and H_2O are located between the negatively charged $Ti_3O_7^{2-}$ layers. The amount of Na^+ in samples which is represented by the value of x in the formula can be controlled by an acid washing process after the hydrothermal reaction. Fig. 2 shows the typical SEM images of TNFs-1, we can see the titanate nanofibers with diameters range of 100–300 nm and lengths several micrometers.

The N_2-BET surface area of TNFs-1 is measured as 203.83 m^2/g and the pore volume is 0.38 cm^3/g. The pore size distribution of TNFs-1 is obtained by BJH method, and it is shown in Fig. 3. As can be seen, the distribution of average pore diameter curve presents a maximum with an average pore diameter of about 3.6 nm. The amount of average pore diameters ranging from 2 nm to 10 nm is predominant. Therefore, TNFs-1 can be considered as mesoporous adsorbents [38].

Table 1
Na amount of TNFs and the effect on Cu(II) removal.

Adsorbent	Na amount (wt.%)	Cu(II) removal (%)
TNFs-1	10.86	97.5
TNFs-2	6.45	81.3
TNFs-3	1.52	23.6
TNFs-4	0.37	10.3

3.2. Effect of Na amount

The Na amount of TNFs-1, TNFs-2, TNFs-3 and TNFs-4 was measured by EDX, and the Cu(II) removal efficiency of each is shown in Table 1. As can be seen, the removal efficiency decreases while the Na amount of TNFs decreases, TNFs-1 with the most of Na amount (10.86%) has the highest Cu(II) removal efficiency, while TNFs-4 with little Na existence has the weakest ability to adsorb Cu(II).

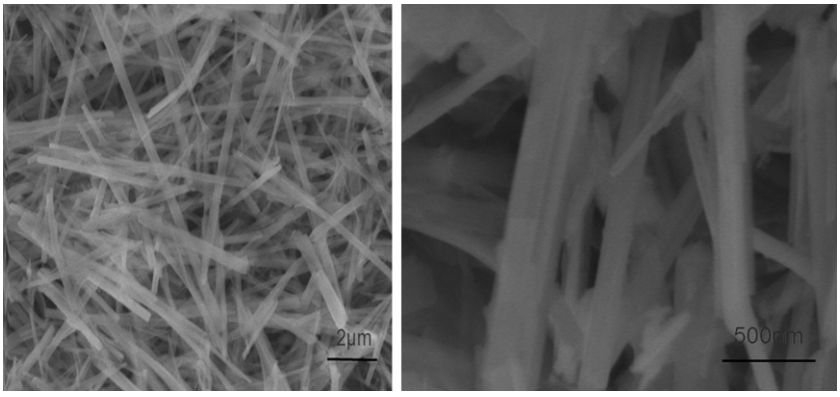

Fig. 2. SEM photographs of TNFs-1.

The Cu(II) removal ability of TNFs is consistent with the Na amount which intensively indicates that Na^+ ions existing in the interlayer of TNFs is a decisive factor of the adsorption. This will be discussed in detail later and TNFs-1 were chosen for further research.

3.3. Effect of pH

The pH of solution is an important variable affecting metal ion adsorption [39]. The pH value affects the surface charge of absorbents, the metal ionization degree and the metal speciation, all of which can affect the adsorption mechanism and the uptake capacity [40]. Table 2 shows the effect of pH on the removal efficiency of Cu(II) ions by TNFs-1. As can be seen, the best pH value for Cu(II) removal is at around 4 (99.8% removal). The adsorption increases abruptly with the increasing pH values from 1 to 4, then decreases gradually at pH > 4.

The effect of pH on the surface charge of adsorbents can be characterized by the values of zeta potential and the measurement results are also shown in Table 2. As we can see, the zeta potential decreases while the pH value increases from 1 to 4 and changes very little at pH > 4. The point of zero charge (PZC) is determined to be about 3.0 and the surface is positively charged at pH < 3.0. Thus, electrostatic repulsion occurs between Cu^{2+} ions and the adsorbent surface at pH < 3.0. Meanwhile, there is a more competitive adsorption between protons and Cu(II) ions at low pH [8]. It is the combination of these factors that results in the lowest removal efficiency observed at pH 1. The increase of adsorption at pH between 1 and 4 can be attributed to the more negatively charged adsorbent surface and to the decrease competitive adsorption by protons.

At pH > 4, the adsorption decreases gradually although the surface charge of TNFs-1 changes very little. This decrease may be caused by the change of copper speciation. Cu(II) species are present in the forms of Cu^{2+}, $Cu(OH)^+$, $Cu_2(OH)_2{}^{2+}$ and $Cu(OH)_2$ at different pH values [41]. The equilibrium equations are listed below:

$$Cu^{2+} + H_2O = Cu(OH)^+ + H^+ \quad (4)$$

$$Cu^{2+} + 2H_2O = Cu(OH)_2 + 2H^+ \quad (5)$$

$$2Cu^{2+} + 2H_2O = Cu_2(OH)_2{}^{2+} + 2H^+ \quad (6)$$

As pH increases, more $Cu(OH)^+$, $Cu_2(OH)_2{}^{2+}$ and insoluble $Cu(OH)_2$ are generated. This may not be favorable change for adsorption, and adsorbents are deteriorated with copper precipitation. Therefore, pH 4 was selected to be the optimum pH for further studies.

3.4. Effect of temperature and thermodynamic study

The study of temperature effect on adsorption was carried out at three different temperatures 30, 45 and 60 °C. The initial Cu(II) concentration was set as 200 mg/l. 50 mg TNFs-1 were mixed with 40 ml Cu(II) solution at pH 4, agitation speed 300 rpm for 6 h. The adsorption capacity is presented in Table 3. The adsorption capacity increases slightly with increasing temperature. As we know, the adsorption capacity increases with temperature with the endothermic reactions and decreases with temperature while the reaction must be exothermic. Hence, the Cu(II) adsorption on TNFs-1 is an endothermic process. Thermodynamic parameters, such as free energy change (ΔG), enthalpy change (ΔH) and entropy change (ΔS) can be calculated by Eqs. (7)–(9) [42]:

$$K_c = \frac{C_{Ae}}{C_e} \quad (7)$$

$$\Delta G = -RT \ \ln K_c \quad (8)$$

$$\log K_c = \frac{\Delta S}{2.303R} - \frac{\Delta H}{2.303RT} \quad (9)$$

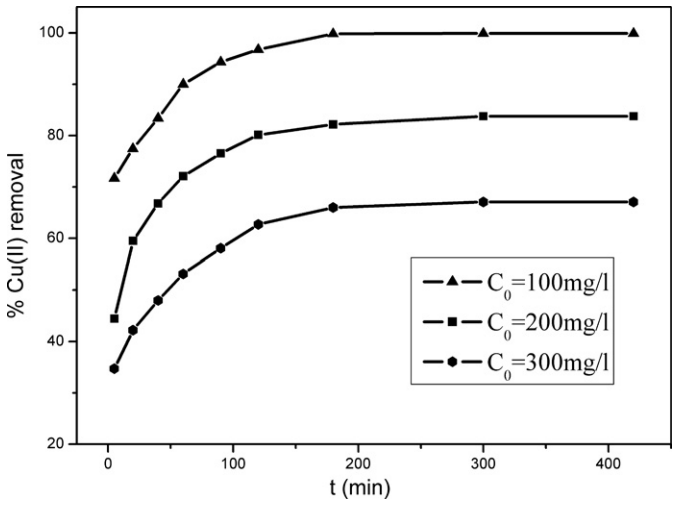

Fig. 4. Effect of contact time on Cu(II) removal (dosage, 1.25 g/l; temperature, 30 °C; agitation speed, 300 rpm; pH 4).

where K_c is the equilibrium constant, C_e is the equilibrium concentration in solution (mg/l) and C_{Ae} is the solid phase concentration at equilibrium (mg/l). The results are calculated and also listed in Table 3. The negative ΔG indicates the adsorption process is spontaneous in nature and positive ΔH confirms it to be endothermic.

Although Cu(II) removal is more efficient at higher temperature, considering the fact that if the adsorbents can be industrial used, an increase in temperature will obviously raises the cost, further studies were still carried out at 30 °C (room temperature).

3.5. Effect of contact time

The contact time needed to reach adsorption equilibrium is another important parameter for adsorbents. The initial concentration range of 100–300 mg/l was used. Cu(II) concentrations were measured at regular intervals and the results are shown in Fig. 4. As can be seen, high removal rate can be observed at the onset (5 min, 71.68% for 100 mg/l, 44.43% for 200 mg/l and 34.72% for 300 mg/l), and then plateau values are gradually reached within 180 min. Finally, 99.8%, 83.75% and 67.05% Cu(II) was adsorbed for each initial concentration. The decreasing concentration of Cu(II) remaining in the solution indicates that Cu(II) is adsorbed by TNFs-1 strongly and quickly. For relatively lower initial concentration 100 mg/l, most of the adsorption happens in the first 5 min and the equilibrium Cu(II) concentration (0.2 mg/l) is in the safe range for drinking which is of interest in terms of both environmental effects and economic effects.

3.6. Effect of initial concentration

The metal adsorption is particularly dependent on initial heavy metal ion concentration. At low concentration values, metals are absorbed by specific sites, while with increasing metal concentration the specific sites are saturated and exchange sites are filled [5]. To study the effect of initial concentration on Cu(II) removal by TNFs-1, a serious of different Cu(II) concentration solutions from 50 mg/l to 600 mg/l were used. The results are presented in Fig. 5. It is shown that the adsorption capacity increases while Cu(II) removal percentage decreases with the increasing initial concentration from 50 mg/l to 600 mg/l. At the beginning of initial concentration (50 mg/l, 100 mg/l and 150 mg/l), the removal percentage is very high (99.8%, 99.8% and 97.9%, respectively) and the adsorption capacity increases linearly. This can be explained by that the adsorption is not saturated at low initial concentration. When

Table 2
Effect of pH on zeta potential of TNFs-1 and on the Cu(II) removal percentage.

	pH values						
	1	2	3	4	5	6	7
Zeta potential (mV)	27.4	19.8	−0.7	−47.7	−43.5	−44.2	−50.7
Cu(II) removal (%)	20.6	37.2	83.1	99.8	97.1	90.6	81.7

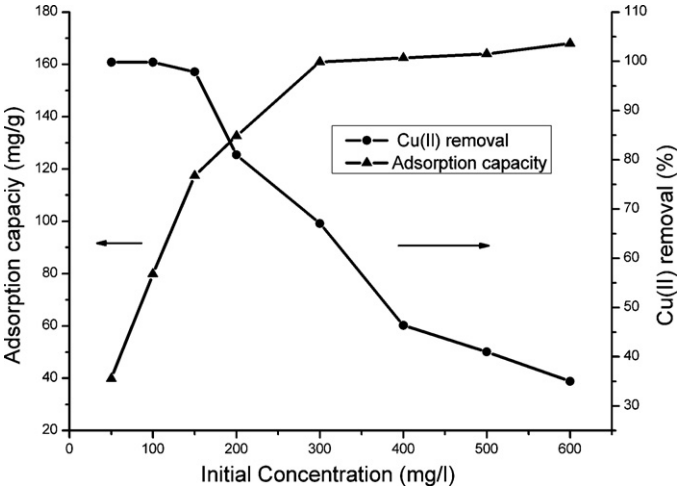

Fig. 5. Effect of initial concentration on Cu(II) removal (dosage, 1.25 g/l; temperature 30 °C; agitation speed, 300 rpm; pH 4).

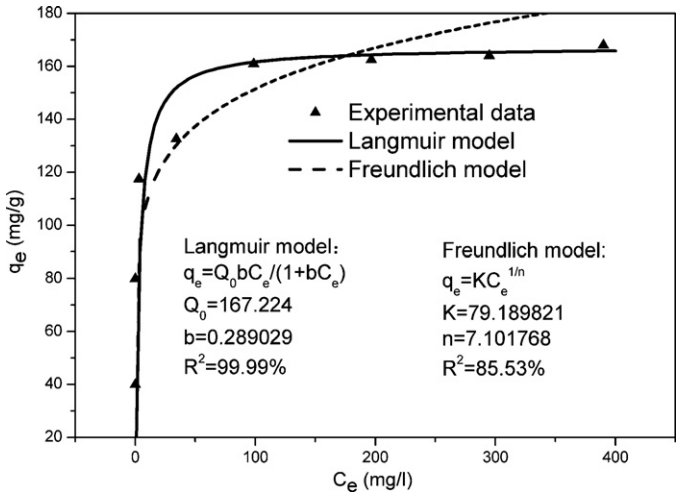

Fig. 6. Adsorption isotherms of Cu(II) removal (dosage, 1.25 g/l; temperature 30 °C; agitation speed, 300 rpm; pH 4).

the initial concentration increases continually, the removal percentage decreases gradually. There is only 35% removal for initial concentration 600 mg/l. At the same time, the adsorption capacity increases until it tends to be a constant with the increasing initial concentration. The constant is the maximum of adsorption capacity which can be calculated by the adsorption isotherm models. At a higher initial concentration, the ratio of initial number of copper ions to the exchangeable sodium ions and the available adsorption surface area is higher, as a result, adsorption percentage is less and adsorption capacity increases until it is saturated. This might be the major mechanism of the effect of the initial Cu(II) concentration on the adsorption process.

3.7. Adsorption isotherm models

The adsorption isotherm is based on the assumption that every adsorption site is equivalent and independent of whether or not adjacent sites are occupied. Isotherms show the relationship between metal concentration in solution and the amount of metal adsorbed on the specific sorbent at a constant temperature [5]. So, the study of adsorption isotherms can help describe the adsorption mechanism. A variety of isotherm models have been used, some of which are more theoretical and some are just empirical. For a newly developed adsorbent, it is important to get a correct equilibrium equation between the solid and liquid phase concentration of Cu(II). In the present study, Langmuir and Freundlich isotherm models are tested with experimental data in Fig. 5. The equations are given as below [43]:

Langmuir equation:

$$q_e = \frac{Q_0 b C_e}{1 + bC_e} \tag{10}$$

Freundlich equations:

$$q_e = kC_e^{1/n} \tag{11}$$

where q_e is the amount of adsorbate adsorbed per unit mass of adsorbent (mg/g), C_e the equilibrium concentration, Q_0 the solid phase concentration corresponding to the complete monolayer coverage of adsorption sites [44], b the constant related to the free energy of adsorption. The constants of k and n in the Freundlich model are related to the strength of the adsorptive bond and the bond distribution [45].

The Langmuir isotherm assumes that the free energy of adsorption does not depend on the surface coverage. It also predicts the solid surface saturation with monolayer coverage of adsorbate at high C_e and a linear adsorption at low C_e values [46]. Freundlich isotherm model assumes that the ratio of the amount of solute adsorbed onto a given mass of adsorbent to the concentration of the solute in the solutions is not constant at different solution concentrations.

The results of adsorption isotherm study are presented in Fig. 6. As can be seen, Langmuir model fits the experimental data very well with the R^2 value 0.9999 and it is much better than the Freundlich model which indicates that Cu(II) ions are adsorbed on TNFs-1 as a monolayer adsorption. The Langmuir constant Q_0, which is a measure of the monolayer adsorption capacity, is obtained as

Table 3
Adsorption capacity at different temperatures and the calculated thermodynamic parameters.

Temperature (K)	Adsorption capacity (mg/g)	ΔG (kJ mol^{-1})	ΔH (kJ mol^{-1})	ΔS (J K^{-1} mol^{-1})
303	132.6	−9.057		
318	135.7	−9.823	6.261	50.57
333	138.1	−10.574		

167.224 mg/g. The essential features of Langmuir isotherm can be expressed in terms of dimensionless constant separation factor (R_L) that can be defined by the following relationship [40]:

$$R_L = \frac{1}{1 + bC_0} \tag{12}$$

where C_0 is the initial concentration (mg/l) and b is the Langmuir constant (l/mg). For $b = 0.289029$, the value of R_L is found in the range of 0.0057 and 0.0647 ($0 < R_L < 1$) which means the adsorption process is always favorable. The values of R_L are near zero which confirms that the adsorption is irreversible [43] and Cu(II) equilibrium concentration can maintain at a low level.

3.8. Adsorption kinetics

To better understand the adsorption process, Lagergren's pseudo-first-order and pseudo-second-order kinetic model are tested in order to predict the adsorption data of Cu(II) as function of time using the data in Fig. 4.

3.8.1. Pseudo-first-order kinetics

Lagergren showed that the rate of adsorption of solute on the adsorbent is based on the adsorption capacity and followed a pseudo-first-order equation [43]. The nonlinear form of the equation is given below:

$$\frac{dq_t}{dt} = k_1(q_e - q_t) \tag{13}$$

where q_e and q_t are the amounts of Cu(II) adsorbed (mg/g) at equilibrium and at any instant time, t, respectively, and k_1 (l/min) is the rate constant of the pseudo-first-order adsorption process. After the application of the initial condition of $q_t = 0$ at $t = 0$, the linear form of the equation is given by Eq. (14):

$$\log(q_e - q_t) = \log\ q_e - \frac{k_1 t}{2.303} \tag{14}$$

The plot of $\log(q_e - q_t)$ versus t gives a straight line for the pseudo-first-order kinetics from which the adsorption rate constant, k_1, is estimated. The values of k_1 and q_e for experimental data in Fig. 4 are calculated and listed in Table 4. The q_e values calculated are not in agreement with experimental data, this is because pseudo-first-order equation is not a true first-order equation [43]. The pseudo-first-model is just used to estimate k_1 which is considered as mass transfer coefficient in the design calculations.

3.8.2. Pseudo-second-order kinetics

As a result of the inapplicability of pseudo-first-order model to estimate q_e, pseudo-second-order kinetics has to be tested for the estimation of q_e. The equation of pseudo-second-order kinetics is given below:

$$\frac{dq_t}{dt} = k_2(q_e - q_t)^2 \tag{15}$$

where k_2 is the second-order rate constant (g/mg min^{-1}). After adding the initial conditions of $t = 0$ to $t = t$ and $q_t = 0$ to $q_t = q_t$, the equation becomes the following linear form:

$$\frac{t}{q_t} = \frac{1}{k_2 q_e^2} + \left(\frac{1}{q_e}\right)t \tag{16}$$

where $k_2 q_e^2$ can be regarded as the initial adsorption rate as $t \to 0$. The plot of t/q_t versus t gives a linear straight as shown in Fig. 7 for the initial Cu(II) concentration range of 100–300 mg/l. From the plot, the values of second-order rate constant k_2, estimated equilibrium adsorption capacity q_e, and the coefficient of determination R^2 are calculated and listed in Table 4. The calculated q_e values show a good agreement with the experimental data and the obtained values for coefficient of determination (R^2) are about 0.999 which indicates that the pseudo-second-order kinetic model describes well the adsorption of Cu(II) using TNFs-1 as adsorbents.

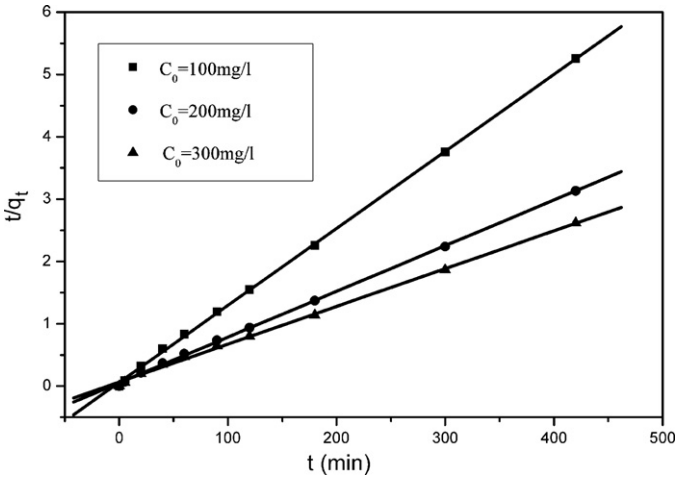

Fig. 7. Pseudo-second-order kinetic plot for the adsorption of Cu(II) (dosage, 1.25 g/l; temperature 30 °C; agitation speed, 300 rpm; pH 4).

3.9. Desorption study

Desorption studies are important since they contribute to elucidate the nature of adsorption process and recover metal ions. Moreover, for potential practical application, it is also important to examine the reusability of adsorbents. In this study, EDTA-2Na solutions with different concentrations were examined to desorb Cu(II) loaded on TNFs-1 and the results are shown in Table 5. As can be seen, the best result for Cu(II) desorption (89.3%) was obtained with 10^{-1} M EDTA-2Na. The regenerated TNFs-1 can still be used for Cu(II) removal and the percentage removal decreased from 99.8% to 92.7% (for initial Cu(II) concentration 100 mg/l) compared to fresh TNFs-1. The mechanism of desorption process may be attributed to the fact that EDTA-2Na can form steady complex with metal ions [47]. And meanwhile, the ionized Na^+ from EDTA-2Na may enter into the interlayer of TNFs-1 while Cu^{2+} was taken out by EDTA-2Na which led to the regeneration of TNFs-1.

3.10. Adsorption mechanism

EDX analysis was performed to determine the chemical composition before and after adsorption. Fig. 8 shows EDX spectrums of TNFs-1 before and after adsorption. The existence of Na, Ti and O elements is revealed in Fig. 8(a). While after the adsorption, there is no Na remaining in TNFs-1 and Cu appears instead, as can be seen in Fig. 8(b). The result indicates that Na^+ ions existing in the interlayer of TNFs-1 are replaced by Cu^{2+} ions in solution through an ion-exchange process during the adsorption. Through the discussion of XRD patterns, the formula of TNFs can be denoted as $Na_xH_{2-x}Ti_3O_7{\cdot}nH_2O$. There is little H^+ existing in TNFs-1, so the ion-exchange between Na^+ in TNFs-1 and Cu^{2+} in solutions can be expressed as:

$$Na_2Ti_3O_7 \cdot nH_2O + Cu^{2+} \overset{\text{ion exchange}}{\longleftrightarrow} CuTi_3O_7 \cdot nH_2O + 2Na^+ \tag{17}$$

The Na content of the TNFs-1 is 10.86% from Table 1, if we assume that all Na^+ ions are replaced by Cu^{2+}, the maximum adsorption capacity of Cu(II) through ion-exchange process is 151.1 mg/g. From the Langmuir isotherm model study, the maximum adsorption capacity is 167.224 mg/g which indicates that ion exchangeable Na^+ between the interlayer is the major reason for adsorption. From the study of Na amount effect on Cu(II) adsorption before, we can draw the same conclusion that Na^+ existing in

Table 4
Pseudo-first-order and pseudo-second-order kinetic parameters for adsorption of Cu(II) onto TNFs-1.

C_0 (mg/l)	q_e(exp) (mg/g)	Pseudo-first-order kinetics			Pseudo-second-order kinetics		
		k_1	q_e	R^2	$k_2 \times 10^3$	q_e	R^2
100	79.8	0.289	74.2	0.9402	2.62	80.9	0.9996
200	132.6	0.129	123.1	0.9267	1.03	136.2	0.9994
300	160.9	0.086	145.1	0.8637	0.57	164.7	0.9982

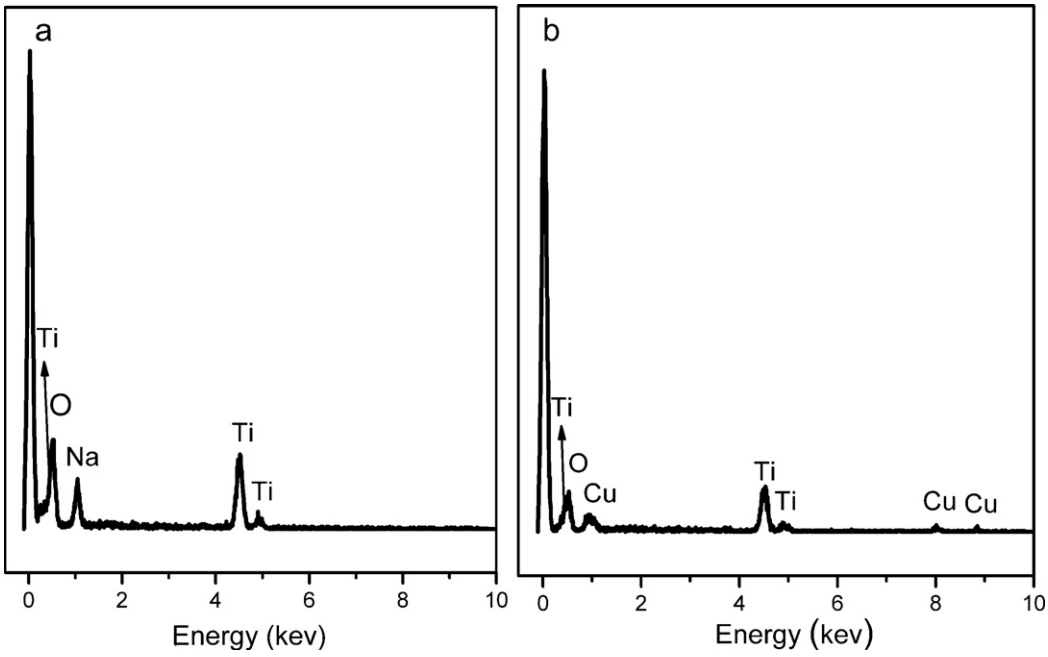

Fig. 8. EDX spectrums of TNF-1 before (a) and after (b) adsorption.

Table 5
Desorption of Cu(II) by EDTA-2Na and Cu(II) adsorption using regenerated TNFs-1.

EDTA-2Na concentration	Desorption percentage (%)	Cu removal by registered TNFs-1 (%)
10^{-1} M	89.3	92.7
10^{-2} M	85.9	86.5
10^{-3} M	76.1	79.2
10^{-4} M	64.7	65.3

the interlayer is essential for adsorption and H^+ in the interlayer cannot be exchanged by Cu^{2+}.

Meanwhile, TNFs-1 possess large negatively charged BET surface area (at pH $\geq$ 3.0) and mesoporous pore structure which makes sure that Cu(II) ions could be physically adsorbed at the surface and provides a pleasant ambience for the ion-exchange between Na^+ and Cu^{2+} ions.

4. Conclusions

In summary, novel low cost adsorbents of titanate nanofibers are prepared by a simple hydrothermal process using inexpensive industrial grade metatitanic acid as raw material. The nanofibers prepared possess large surface area, mesoporous pore structure and ion-exchange ability. The batch experimental results suggest that the adsorption of Cu(II) onto nanofibers is particularly dependent on solution pH and Na amount of adsorbents. Cu(II) removal by TNFs-1 is highly effective and the efficiency can reach 99.8% for initial concentration 100 mg/l under optimal conditions. The concentration of Cu(II) remaining in solution after adsorption can maintain at a low level which is in safe range for drinking water usage. The rate for Cu(II) adsorption is rapid, most of the adsorption happens in the first 5 min and equilibrium can be gradually reached within 180 min.

Equilibrium adsorption follows Langmuir isotherms well and the maximum Cu(II) uptake calculated is 167.224 mg/g which is much better than many other low-cost and commercially available adsorbents. Thermodynamics study shows the adsorption is spontaneous and endothermic. The kinetics of adsorption for different Cu(II) initial concentrations is explained by pseudo-second-order kinetic model. The Cu-loaded adsorbents are regenerated by EDTA-2Na solutions and the EDX spectrums show that the adsorption is mainly based on ion-exchange mechanism.

As a consequence, there is no denying that this work has provide a new candidate of adsorbent for the removal of heavy metal ions like Cu(II) ions from wastewater. The TNFs-1 have the potential to be used both for trace level heavy metal removal in drinking water purification and for high concentrated industrial wastewater treatment.

Acknowledgement

This work was financially supported by a grant from the National Basic Research Program of China (No. 2011CB933700).

References

[1] T. Gotoh, K. Matsushima, K.I. Kikuchi, Preparation of alginate–chitosan hybrid gel beads and adsorption of divalent metal ions, Chemosphere 55 (2004) 135–140.

[2] Y. Sag, Y. Aktay, Kinetic studies on sorption of Cr(VI) and Cu(II) ions by chitin, chitosan and Rhizopus arrhizus, Biochem. Eng. J. 12 (2002) 143–153.
[3] K.C. Justi, V.T. Favere, M.C.M. Laranjeira, A. Neves, R.A. Peralta, Kinetics and equilibrium adsorption of Cu(II), Cd(II), and Ni(II) ions by chitosan functionalized with 2-bis-(pyridylmethyl)aminomethyl-4-methyl-6-formylphenol, J. Colloid Interface Sci. 291 (2005) 369–374.
[4] A. Sari, M. Tuzen, D. Citak, M. Soylak, Adsorption characteristics of Cu(II) and Pb(II) onto expanded perlite from aqueous solution, J. Hazard. Mater. 148 (2007) 387–394.
[5] M.S. Rahman, M.R. Islam, Effects of pH on isotherms modeling for Cu(II) ions adsorption using maple wood sawdust, Chem. Eng. J. 149 (2009) 273–280.
[6] Ministry of Health of P.R. China and Standardization Administration of P.R. China, Sanitary Standard for Drinking Water (GB5749-2006), 2007.
[7] N. Chiron, R. Guilet, E. Deydier, Adsorption of Cu(II) and Pb(II) onto a grafted silica: isotherms and kinetic models, Water Res. 37 (2003) 3079–3086.
[8] S. Liang, X. Guo, N. Feng, Q. Tian, Isotherms, kinetics and thermodynamic studies of adsorption of Cu^{2+} from aqueous solutions by Mg^{2+}/K^{+} type orange peel adsorbents, J. Hazard. Mater. 174 (2010) 756–762.
[9] Y.T. Zhou, C. Branford-White, H.L. Nie, L.M. Zhu, Adsorption mechanism of Cu^{2+} from aqueous solution by chitosan-coated magnetic nanoparticles modified with alpha-ketoglutaric acid, Colloid Surf. B 74 (2009) 244–252.
[10] D.J. Malik, V. Strelko, M. Streat, A.M. Puziy, Characterisation of novel modified active carbons and marine algal biomass for the selective adsorption of lead, Water Res. 36 (2002) 1527–1538.
[11] M.J.S. Yabe, E. de Oliveira, Heavy metals removal in industrial effluents by sequential adsorbent treatment, Adv. Environ. Res. 7 (2003) 263–272.
[12] C. Tiffreau, J. Lützenkirchen, P. Behar, Modelling the adsorption of mercury(II) and (hydroxides). Part I. Amorphous ions oxides and alpha quartz, J. Colloid Interface Sci. 172 (1995) 82–93.
[13] J. Wang, C. Chen, Biosorbents for heavy metals removal and their future, Biotechnol. Adv. 27 (2009) 195–226.
[14] L.D. Zhang, M. Fang, Nanomaterials in pollution trace detection and environmental improvement, Nano Today 5 (2010) 128–142.
[15] T. Kasuga, M. Hiramatsu, A. Hoson, T. Sekino, K. Niihara, Formation of titanium oxide nanotube, Langmuir 14 (1998) 3160–3163.
[16] T. Kasuga, M. Hiramatsu, A. Hoson, T. Sekino, K. Niihara, Titania nanotubes prepared by chemical processing, Adv. Mater. 11 (1999) 1307–1311.
[17] X.M. Sun, Y.D. Li, Synthesis and characterization of ion-exchangeable titanate nanotubes, Chem. Eur. J. 9 (2003) 2229–2238.
[18] Z.Y. Yuan, B.L. Su, Titanium oxide nanotubes, nanofibers and nanowires, Colloids Surf. A 241 (2004) 173–183.
[19] S.V.N.T. Kuchibhatla, A.S. Karakoti, D. Bera, S. Seal, Seal, One dimensional nanostructured materials, Prog. Mater. Sci. 52 (2007) 699–913.
[20] Z.H. Zhang, X.H. Zhong, S.H. Liu, D.F. Li, M.Y. Han, Aminolysis route to monodisperse titania nanorods with tunable aspect ratio, Angew. Chem. Int. Ed. 44 (2005) 3466–3470.
[21] Y.N. Zhao, J. Jun, Y. Xiaoqin, Hydrothermal synthesis of titanate nanowire arrays, Mater. Lett. 61 (2007) 384–388.
[22] D.V. Bavykin, J.M. Friedrich, F.C. Walsh, Protonated titanates and TiO_2 nanostructured materials: synthesis, properties, and applications, Adv. Mater. 18 (2006) 2807–2824.
[23] H.H. Ou, S.L. Lo, Review of titania nanotubes synthesized via the hydrothermal treatment: fabrication, modification, and application, Sep. Purif. Technol. 58 (2007) 179–191.
[24] C.H. Lin, C.H. Lee, J.H. Chao, C.Y. Kuo, Y.C. Cheng, W.N. Huang, H.W. Chang, Y.M. Huang, M.K. Shih, Photocatalytic generation of H-2 gas from neat ethanol over Pt/TiO_2 nanotube catalysts, Catal. Lett. 98 (2004) 61–66.
[25] M. Hodos, E. Horvath, H. Haspel, A. Kukovecz, Z. Konya, I. Kiricsi, Photo sensitization of ion-exchangeable titanate nanotubes by CdS nanoparticles, Chem. Phys. Lett. 399 (2004) 512–515.
[26] S.H. Lim, J.Z. Luo, Z.Y. Zhong, W. Ji, J.Y. Lin, Room-temperature hydrogen uptake by TiO_2 nanotubes, Inorg. Chem. 44 (2005) 4124–4126.
[27] Y.K. Zhou, L. Cao, F.B. Zhang, B.L. He, H.L. Li, Lithium insertion into TiO_2 nanotube prepared by the hydrothermal process, J. Electrochem. Soc. 150 (2003) 1246–1249.
[28] A.R. Armstrong, G. Armstrong, J. Canales, P.G. Bruce, TiO_2-B nanowires as negative electrodes for rechargeable lithium batteries, J. Power Sources 146 (2005) 501–506.
[29] S. Kim, H. Park, C. Kwak, M. Ji, M. Lee, J. Paik, B. Choi, Characterization of pore structure of mesoporous hydrogen titanium oxide hydrates, J. Phys. Chem. Solids 69 (2008) 1139–1141.
[30] Y.C. Chen, S.L. Lo, J. Kuo, Pb(II) adsorption capacity and behavior of titanate nanotubes made by microwave hydrothermal method, Colloids Surf. A 361 (2010) 126–131.
[31] S.S. Liu, C.K. Lee, H.C. Chen, C.C. Wang, L.C. Juang, Application of titanate nanotubes for Cu(II) ions adsorptive removal from aqueous solution, Chem. Eng. J. (2009) 188–193.
[32] H.Y. Niu, J.M. Wang, Y.L. Shi, Y.Q. Cai, F.S. Wei, Adsorption behavior of arsenic onto protonated titanate nanotubes prepared via hydrothermal method, Micropor. Mesopor. Mater. 122 (2009) 28–35.
[33] H.Y. Zhu, Y. Lan, X.P. Gao, S.P. Ringer, Z.F. Zheng, D.Y. Song, J.C. Zhao, Phase transition between nanostructures of titanate and titanium dioxides via simple wet-chemical reactions, J. Am. Chem. Soc. 127 (2005) 6730–6736.
[34] E. Morgado, M.A.S. de Abreu, G.T. Moure, B.A. Marinkovic, P.M. Jardim, A.S. Araujo, Characterization of nanostructured titanates obtained by alkali treatment of TiO_2-anatases with distinct crystal sizes, Chem. Mater. 19 (2007) 665–676.
[35] E. Morgado, M.A.S. de Abreu, O.R.C. Pravia, B.A. Marinkovic, P.M. Jardim, F.C. Rizzo, A.S. Araujo, A study on the structure and thermal stability of titanate nanotubes as a function of sodium content, Solid State Sci. 8 (2006) 888–900.
[36] Y. Suzuki, S. Yoshikawa, Synthesis and thermal analyses of TiO_2-derived nanotubes prepared by the hydrothermal method, J. Mater. Res. 19 (2004) 982–985.
[37] O.P. Ferreira, A.G. Souza, J. Mendes, O.L. Alves, Unveiling the structure and composition of titanium oxide nanotubes through ion exchange chemical reactions and thermal decomposition processes, J. Braz. Chem. Soc. 17 (2006) 393–402.
[38] J.C.P. Vaghetti, E.C. Lima, B. Royer, J.L. Brasil, B.M. da Cunha, N.M. Simon, N.F. Cardoso, C.R.Z. Norena, Application of Brazilian-pine fruit coat as a biosorbent to removal of Cr(VI) from aqueous solution—kinetics and equilibrium study, Biochem. Eng. J. 42 (2008) 67–76.
[39] A.R. Iftikhar, H.N. Bhatti, M.A. Hanif, R. Nadeem, Kinetic and thermodynamic aspects of Cu(II) and Cr(III) removal from aqueous solutions using rose waste biomass, J. Hazard. Mater. 161 (2009) 941–947.
[40] S. Babel, T.A. Kurniawan, Cr(VI) removal from synthetic wastewater using coconut shell charcoal and commercial activated carbon modified with oxidizing agents and/or chitosan, Chemosphere 54 (2004) 951–967.
[41] J.X. Li, J. Hu, G.D. Sheng, G.X. Zhao, Q. Huang, Effect of pH, ionic strength, foreign ions and temperature on the adsorption of Cu(II) from aqueous solution to GMZ bentonite, Colloids Surf. A (2009) 195–201.
[42] T.H. Shi, Z.C. Wang, Y. Liu, S.G. Jia, D. Changming, Removal of hexavalent chromium from aqueous solutions by D301, D314 and D354 anion-exchange resins, J. Hazard. Mater. 161 (2009) 900–906.
[43] S. Gupta, B.V. Babu, Removal of toxic metal Cr(VI) from aqueous solutions using sawdust as adsorbent: equilibrium, kinetics and regeneration studies, Chem. Eng. J. 150 (2009) 352–365.
[44] C.P. Huang, E.H. Smith, Removal of Cd(II) from plating wastewater by an activated carbon process, Chem. Water Reuse 2 (1981) 355–398.
[45] V.K. Gupta, S. Sharma, I.S. Yadau, M. Dinesh, Utilisation of bagasses fly ash generated in sugar industry for the removal of phenol and p-nitrophenol from wastewater, J. Chem. Technol. Biotechnol. 71 (1998) 180–186.
[46] L. Khezami, R. Capart, Removal of chromium(VI) from aqueous solution by activated carbons: kinetic and equilibrium studies, J. Hazard. Mater. 123 (2005) 223–231.
[47] W. Shen, S.Y. Chen, S.K. Shi, X. Li, X. Zhang, W.L. Hu, H.P. Wang, Adsorption of Cu(II) and Pb(II) onto diethylenetriamine-bacterial cellulose, Carbohydr. Polym. 75 (2009) 110–114.